

## Flow Past An Impulsively Started Oscillating Elliptical Cylinder

T.L. Chng, T. T. Lim, J. Soria<sup>1</sup>, K. B. Lua and K. S. Yeo

Fluid Division, Department of Mechanical Engineering,  
National University of Singapore,

10 Kent Ridge Crescent, Singapore 119260.

<sup>1</sup>LTRAC, Monash University, Melbourne, Victoria 3800, Australia.

### Abstract

The current experimental study on a two-dimensional oscillating aerofoil aims to isolate and explore the effects of wing twisting, one of the most basic aspects of insect locomotion. Particle Image Velocimetry (PIV) is employed to study the effects of reduced frequency as well as angular amplitude on an impulsively started aerofoil oscillating which is initially at rest. The forced oscillation is of a sinusoidal nature about a mid-chord, spanwise axis and all investigations are carried out at a Reynolds number of 1000, with amplitudes in the range of 20° to 60°, typical of the regime that insects tend to operate within. A piston tank facility is used to generate the impulsively started motion. The ensemble averaged results obtained suggest that both the reduced frequency and angular amplitude are important governing parameters which influence the development of leading edge structures and subsequent wake vortices. In the limiting case (i.e. fixed angle of attack), the resulting flow field is one fairly similar to that of a bluff body, with the distinct, periodic formation of a von Karman vortex street. In the lower reduced frequency cases, the flow displays characteristics similar to the former, except that the effect of the aerofoil oscillation imposes a velocity component on the flow which seems to retard the leading edge separation. In contrast, in the higher reduced frequency cases, where the velocity component imparted by the oscillatory motion is much higher than that of the freestream, the effect of the freestream velocity seems to be almost non-existent. Vortices are generated in an anti-symmetric manner at both the leading and trailing edges, but whilst the trailing edge vortices are advected downstream, the leading edge vortices are negated before advection can occur.

### Introduction

Over the past two decades, the advancement of non-intrusive experimental techniques and DNS solvers has given scientists the impetus to undertake the study of unsteady aerodynamic problems with newfound resolve. Peculiar to this class of flows is the topic of oscillating aerofoils. Traditionally one which has been applied to flutter analysis, gust response and regarded as a possible avenue of alternative thrust production, this field has incited renewed interest due to its applications to aircraft maneuverability and relevance to insect flight.

From the perspective of the former, the attractiveness of a pitching aerofoil mainly stems from the fact that studies have shown that such a motion is able to generate high levels of lift even when operating beyond the stall angle [1]-[3]. This phenomenon is very similar to the lift overshoot observed during the nascent stages of the flow past a fixed incidence aerofoil [4]. Yet, from a totally different dimension, wing oscillation has also been known to be an integral part of insect wing motion. In recent times, scientists have begun to explore the possibility of applying this concept of dynamic wing motion to future Micro Aviation Vehicles (MAVs). This has in turn contributed to a surge in studies hoping to piece together a sufficiently workable model of insect flight which can subsequently be applied to these man-made vehicles [5]-[6].

Fundamentally speaking, the investigation of both these applications primarily differs in the incidence angles and the Reynolds number regimes that they operate in. Whilst

conventional aerodynamic applications usually span the order of  $10^6$ - $10^8$ , insect flight is centred around a relatively lower range of  $10$ - $10^4$ . Additionally, insects typically flap their wings at mean angles of attack in excess of 40° [7], well within the deep stall regime of most aircraft.

The focus of the current study is on the flow past an impulsively started elliptical cylinder subjected to a sinusoidal oscillation at a nominal Reynolds number of 1000. Such a configuration is aimed at mimicking the twisting motion of an insect wing, one of the basic elements of insect flight. Whilst attempts have been made at producing dynamically scaled models to study the motion of such creatures in their entirety [8], here our emphasis is on examining the artefacts of wing twisting in isolation. Particle Image Velocimetry (PIV) is employed to study the effects of the reduced frequency and angular amplitude on the flow. For the purpose of comparison, the flow past an elliptical cylinder at fixed incidences is also investigated.

Extensive flow visualization studies have previously been conducted to examine the effect of parameters such as the reduced frequency and angular amplitude on the flow field of an oscillating aerofoil [9, 10]. The reduced frequency has generally been found to have a more pronounced effect on the evolving flow structures compared to other parameters like the angular amplitude. In addition, studies have also found that the flow field of an oscillating aerofoil at low reduced frequencies is very similar to that of an aerofoil in static stall whilst at higher reduced frequencies, the flow is primarily due to the rotational motion of the wing. Computational studies have also shown good agreement with the above [11, 12].

### Experimental Setup

The experiments were carried out in a piston tank facility shown in figure 1. The entire setup consists of a stepper motor-driven square piston used to generate the impulsively started flow, and an additional stepper motor used to generate the sinusoidal oscillation. The test section has a square cross section of 198mm by 198mm and a length of about 400mm. In addition, the motion of the piston is restricted to a maximum horizontal displacement of 300mm.

An elliptical cylinder made of brass, with a chord of 60mm, thickness 7.5mm and aspect ratio of 3.25, is used throughout the experiments and spans the entire width of the water tunnel.

A Nd:YAG laser capable of generating 2x300mJ pulses of 5ns duration is used as the illumination source, and produces a uniform light sheet of 2mm thickness. Polyamide particles with a mean diameter of 20µm are used to seed the flow. Images are captured via a 12 bit digital CCD camera with a 1280px by 1024px resolution.

The stepper motors, CCD camera and laser are all computer controlled and linked via an Ethernet interface. TTL signals are used to synchronize all the devices and ensure that they are triggered off simultaneously.

A multigrid cross correlation digital PIV (MCCDPIV) algorithm [13] is used to analyse and process the captured single exposed images. Data validation is carried out using three techniques, the global histogram test, median value operator test and the dynamic mean value operator test. A velocity vector is rejected unless all the criteria are met.

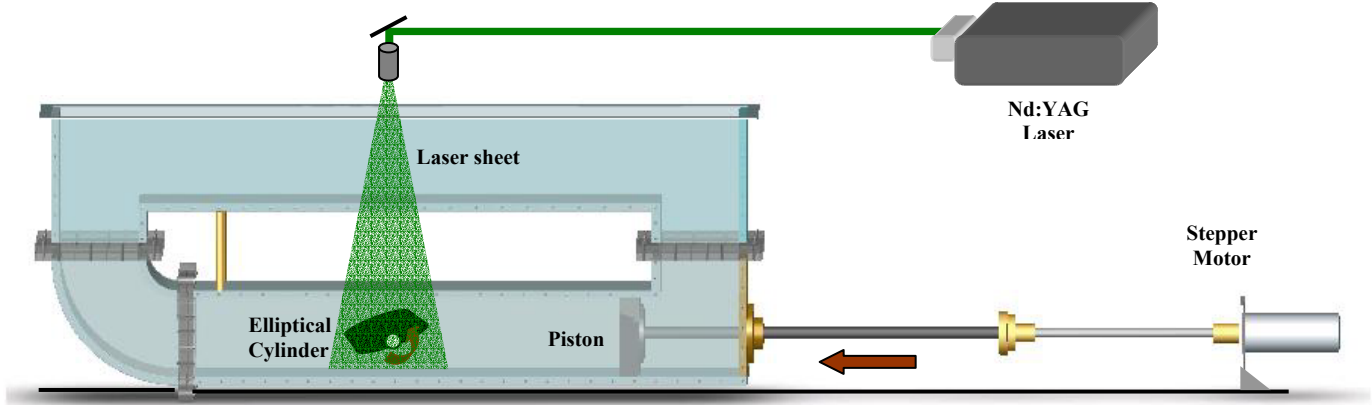


Figure 1: Schematic of piston tank facility.

The opacity of the elliptical cylinder results in a lack of illumination beneath the wing. In order to obtain a complete field of data, two sets of experiments are performed: one with the orientation and motion of the wing reversed and the other as per normal. The two datasets are then merged together. Each realization is repeated a total of 100 times and ensemble averaging is performed.

### Experimental Conditions

For all experiments conducted, the flow is impulsively started from rest with an initial linear acceleration,  $a_0$ , of  $100\text{mm/s}^2$ . The Reynolds number,  $Re$ , is defined as

$$Re = \frac{U_\infty c}{\nu} \quad (1)$$

where  $U_\infty$  is the constant, post acceleration, freestream velocity,  $c$  is the aerofoil chord and  $\nu$  is the kinematic viscosity of water.

For the oscillatory cases, the imposed oscillation is that of a sinusoidal nature, given by the equation:

$$\theta = \theta_0 \sin \omega t \quad (2)$$

where  $\theta$  is the angular displacement,  $\theta_0$  the angular amplitude,  $\omega$  the temporal frequency of oscillation and  $t$  is the time elapsed. The varied parameters are the angular amplitude,  $\theta_0$ , and the oscillation frequency, which is represented by the dimensionless reduced frequency,  $\kappa$ . The reduced frequency is defined as,

$$\kappa = \frac{fc}{2U_\infty} \quad (3)$$

where  $f = \omega/2\pi$  is the oscillation frequency. The time elapsed is also non-dimensionalized by the freestream velocity and aerofoil chord to give,

$$t^* = \frac{tU_\infty}{c} \quad (4)$$

## Results & Discussion

### Fixed Incidence Case

The case of an elliptical aerofoil at a fixed incidence of  $40^\circ$  is presented here for reference. The flow is impulsively started from rest and attains a constant velocity corresponding to a Reynolds number of 1000 at  $t^*=0.048$ . The PIV results reveal a flow field typical of an aerofoil in deep stall. During the initial stages of the flow, a starting vortex is seen to emanate from the trailing edge of the wing. This is accompanied by a corresponding separation at the leading edge which culminates in the formation of the well-known leading edge vortex or separation bubble. The consequent flow is then characterized by shear layer instabilities of a Helmholtz nature just above the leading edge, which result in the eventual shedding of the leading edge vortex. At the same time, the flow is marked by the growth of a secondary vortex, opposite in sign to that of the leading edge vortex, at around the quarter chord position. One possibly attributes the occurrence of this vortex to the adverse pressure

gradient encountered by the flow entrained by the leading edge vortex. Figure 2 clearly shows the presence of this secondary vortex as well as the growth of a new leading edge vortex. Finally, as the initial leading edge vortex is advected downstream beyond the visual field, the growth of a vortex at the trailing edge marks the development of a periodic von Karman vortex street often associated with bluff bodies.

### Oscillatory Case: $\kappa = 0.1$ , $\theta_0 = 40^\circ$

An investigation is carried out for two different reduced frequencies of  $\kappa=0.1$  and  $\kappa=0.5$ , both with a corresponding angular amplitude of  $40^\circ$ .

The lower reduced frequency configuration results in a flow field which is distinguished by its resemblance to the static case described above. The vortical structures such as the initial starting vortex as well as the consequent growth of the leading edge and secondary vortex are all similarly observed (see figure 3A). However, a few differences are worthy of mention. The rotational velocity imposed by the sinusoidal oscillation appears to inhibit the separation characteristics of the aerofoil. Primarily, one observes a delay in the formation of the leading edge vortex during the pitching up motion which is in good agreement with other studies. Similarly, apart from the initial starting vortex, the shedding of trailing edge vortices seems to be practically negated, and is instead replaced by a wavy-like structure. In addition, the pitching motion of the aerofoil repositions both the leading edge and secondary vortex, which traverse the top surface of the aerofoil and are shed into the wake during the course of an oscillation cycle.

### Oscillatory Case: $\kappa = 0.5$ , $\theta_0 = 40^\circ$

In contrast to the above case where the translational flow seems to adapt fairly well to the variation in incidence, the flow pattern for the reduced frequency of  $\kappa=0.5$  is dominated by the rotational motion of the aerofoil. This is due to the fact that the tip velocities of the aerofoil are much larger than that of the freestream. As such, vortices are generated in an anti-symmetric manner as shown in figure 3B, with the growth of secondary vortices perceptibly missing. Also, it is interesting to note that the vortices produced in the vicinity of the leading edge are not advected downstream as in the previous cases. The low pressure region at the leading edge caused by the forceful pitching motion seems to provide a suction effect which prevents these vortices from moving downstream. These vortices are then periodically annihilated during the ensuing motions of the aerofoil. It is also observed that the wake is characterized by the formation of a reverse von Karman jet structure due to the shedding of trailing edge vortices.

### Oscillatory Case: $\kappa = 0.5$ , $\theta_0 = 20^\circ$

A brief investigation of the effect of angular amplitude is conducted for the case of  $\kappa=0.5$ , with  $\theta_0=20^\circ$ . Interestingly, the results display a combination of characteristics of both the oscillatory cases mentioned above. The leading edge vortices are

repositioned by the aerofoil and shed downstream whilst the trailing edge vortices form a reverse von Karman street (see figure 3C).

The foregoing discussion suggests that the ratio of the maximum tip velocity of the aerofoil to that of the freestream plays an important role in determining the characteristics of the flow. More specifically, this dimensionless number establishes the degree of modification of the effective angle of attack at the leading edge. This is evident in a comparison of the two different reduced frequency cases shown in figures 3A and 3B. In the case of the former, the additional velocity component imparted by the aerofoil oscillation is small and only serves to retard the flow evolution characteristics. However, its influence in the latter case is much larger and the flow is virtually dictated by the oscillatory motion.

To a certain extent, the reduced frequency as defined in this study provides a reasonable approximation for this ratio, but a more accurate representation of the aerofoil tip velocity should include the angular amplitude and account for any differences in the location of the pitching axis.

### Concluding Remarks

A preliminary study of an impulsively started elliptical cylinder in oscillatory motion has been conducted. The results show that the ratio of the aerofoil tip velocity to that of the freestream is the main parameter which governs the flow. When this ratio is small, as in the reduced frequency case of  $\kappa=0.1$ , the flow continues to display characteristics reminiscent of an aerofoil in static stall, albeit with a delay in the separation at the leading edge during the pitch up motion. This brings to mind the classical, linearized theory of oscillating aerofoils which predicts that the solutions of an aerofoil conducting small amplitude oscillations are merely functions of the static cases with a certain phase difference.

When this ratio is large, the flow is dominated by the pitching motions of the aerofoil and characterized by the formation of a reverse Von Karman vortex street. Although the reduced frequency provides a reasonable estimate of this ratio, it is proposed that a more complete representation should include the angular amplitude of the oscillation, as well as the location of the pitching axis.

### References

[1] Visbal, M. R. & Shang, J. S., Investigation of the Flow Structure Around a Rapidly Pitching Airfoil, *AIAA J.*, **27**, 1989, 1044-1051.

[2] Currier, J. M. & Fung, K. Y., Analysis of the Onset of Dynamic Stall, *AIAA J.*, **30**, 1992, 2469-2477.  
 [3] Chandrasekhara, M. S., Carr, L. W. & Wilder, M. C., Interferometric Investigations of Compressible Dynamic Stall Over a Transiently Pitching Airfoil, *AIAA J.*, **32**, 1994, 586-593.  
 [4] Katz, J., Yon, S. & Rogers, S. E., Impulsive Start of a Symmetric Airfoil at High Angle of Attack, *AIAA J.*, **34**, 1996, 225-230.  
 [5] Ellington, C. P., The Novel Aerodynamics of Insect Flight: Applications to Micro-air Vehicles, *J. Exp. Bio.*, **202**, 1999, 3439-3448.  
 [6] Sane, S. P. & Dickinson, M. H., The Aerodynamic Effects of Wing Rotation and a Revised Quasi-steady Model of Flapping Flight, *J. Exp. Bio.*, **205**, 2002, 1087-1096.  
 [7] Willmott, A. P. & Ellington, C. P., The Mechanics of Flight in the Hawkmoth *Manduca Sexta*. I. Kinematics of Hovering and Forward Flight, *J. Exp. Bio.*, **200**, 1997, 2705-2722.  
 [8] Ellington, C. P., Berg, C. V., Willmott, A. P. & Thomas, L. R., Leading-edge Vortices in Insect Flight, *Nature*, **384**, 1996, 626-630.  
 [9] Ohmi, K., Coutanceau, M., Loc, T. P. & Dulieu, A., Vortex Formation Around an Oscillating and Translating Airfoil at Large Incidences, *J. Fluid Mech.*, **211**, 1990, 37-60.  
 [10] Ohmi, K., Coutanceau, M., Daube, O. & Loc, T. P., Further Experiments on Vortex Formation Around an Oscillating and Translating Airfoil at Large Incidences, *J. Fluid Mech.*, **211**, 1990, 37-60.  
 [11] D'Alessio, S. J. D., Dennis, S. C. R. & Nguyen, P., Unsteady Viscous Flow Past an Impulsively Started Oscillating and Translating Elliptic Cylinder, *J. Eng. Math.*, **35**, 1999, 339-357.  
 [12] Akbari, M. H. & Price, S. J., Simulation of the Flow Over Elliptic Airfoils Oscillating at Large Angles of Attack, *J. Fluid & Struct.*, **14**, 2000, 757-777.  
 [13] Soria J., Lim, T. T., Hou K. C. & Sengupta T. K., Investigation of Accelerated Flow over an Airfoil at an Angle of Attack using Multigrid Cross-Correlation Digital PIV, *4th International Symposium on Particle Image Velocimetry*, 2001.

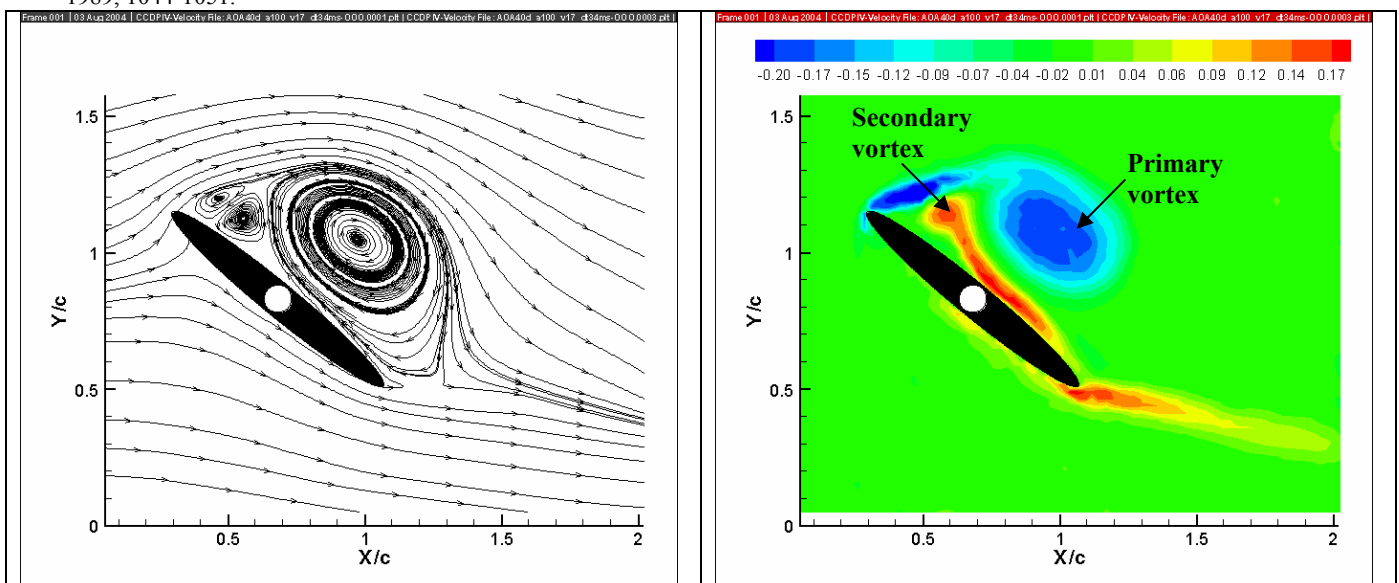


Figure 2: Streamline and vorticity plots for an elliptical aerofoil at  $40^\circ$  incidence,  $Re=1000$ ,  $t^*=1.7$ . Flow is from left to right.

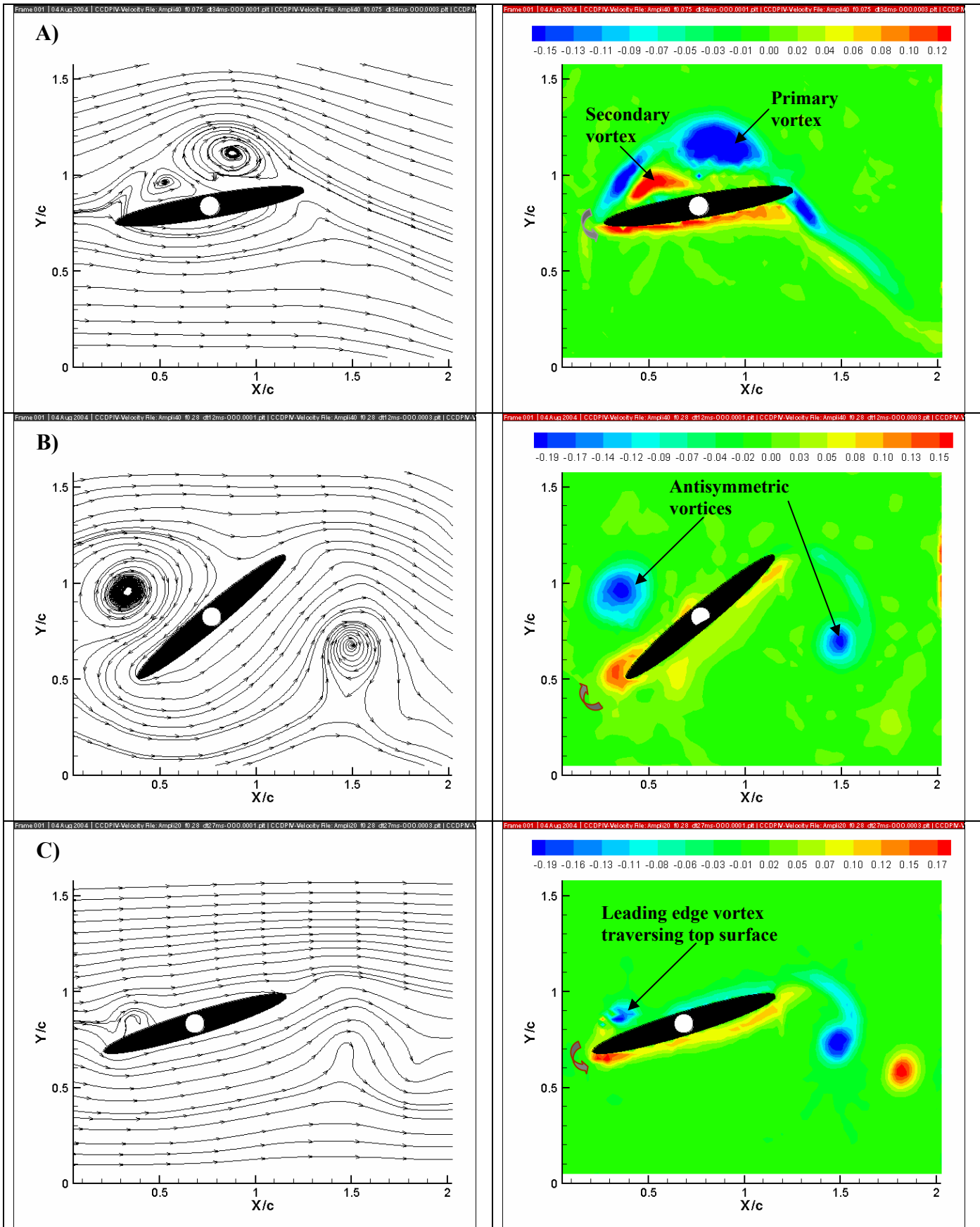


Figure 3: Streamline and vorticity plots for an elliptical aerofoil in sinusoidal oscillation. A)  $Re=1000$ ,  $\kappa=0.1$ ,  $\theta_0=40^\circ$ ,  $\theta=-10^\circ$ ,  $t^*=2.04$ . B)  $Re=1000$ ,  $\kappa=0.5$ ,  $\theta_0=40^\circ$ ,  $\theta=-40^\circ$ ,  $t^*=1.76$ . C)  $Re=1000$ ,  $\kappa=0.5$ ,  $\theta_0=20^\circ$ ,  $\theta=-17^\circ$ ,  $t^*=0.85$ .